A Study on the Phenomenon of Chip Breaking by Computer Analysis

Jeong-du Kim and Eun-sang Lee

Chip breaker selection analysis, possible only through an experimental process, was obtained by a generalized equation that used an orthogonal cutting model and basic chip deformation.

It could analyze the chip breaking phenomena without the use of an actual experimental method, and it was applied to computer simulation and proved the propriety of the theory through actual experiments. It derived the optimum conditions for chip breaking by applying the optimized theory to the basic program. A finite-element model for simulating chip breaking in orthogonal cutting was developed and discussed. By simulation, animation of the chip breaking process was observed on a computer screen.

Keywords:
animation, attached type chip breaker, chip breaking, equivalent stress, finite element modeling, Von Mises yield criterion

1. Introduction

WITH the present development toward automation and unmanned machining, efficient control of the chip breaking process is important. Nakayama[1,2] studied the force acting on a chip breaker in 1962, which showed the ideal chip breaker in machining and reported on a method that described chip control, chip form classification, and chip breaking in 1984. Recently, they have studied chip form and control of chip flow during turning, boring, drilling, etc. Kloor[3] reported on a monitoring system using Sound Detection and Ranging (SODAR) for the detection of unbroken chips. Using a computer, Katbi[4] designed a chip breaker that has the complex form of a groove. The current study theoretically investigated the shear angle and chip radius caused by the chip breaker and derived the linear equation by experimental data. It gradiantly simulated the type of chip possible, observed on a personal computer screen, that was made during these processes. Finally, using data that were obtained from simulation, it attempted to analyze the stress distribution at chip breaking by the finite-element method.

2. Basic Aspects of Chip Breaking

2.1. *Orthogonal Cutting Model* [5]

The cutting ratio and shear angle in orthogonal cutting is as follows:

$$r = t_o / t_c = \sin\varphi / \cos(\varphi - \alpha) \quad [1]$$

$$\tan\varphi = r \times \cos\alpha / (1 - r \times \sin\alpha) \quad [2]$$

Jeong-du Kim and **Eun-sang Lee,** Dept. of Precision Engineering & Mechatronics, Korea Advanced Institute of Science & Technology, Taejon, Korea.

If the volume is not changed in a shear plane for each velocity component:

$$V \times t_o = V_c \times t_c$$

or

$$V_c = V \times r \quad [3]$$

Equations 1 to 3 indicate that the shear angle φ is a function of t_o, t_c, α, V_c, or V; φ is a function of t_o, t_c, α (in Eq 2); and r is the function of V_c and V. Consequently, the shear angle φ can be obtained under given conditions if some variables are known.

2.2. *Chip Breaker*

2.2.1. *Attached Type*

Figure 1 shows the chip formation caused by use of an attached-type chip breaker. The chip radius can be obtained by the following two equations:

$$R = [(l_n - l_f) - (h \times \cot b)] \times \cot(b/2) \quad [4]$$

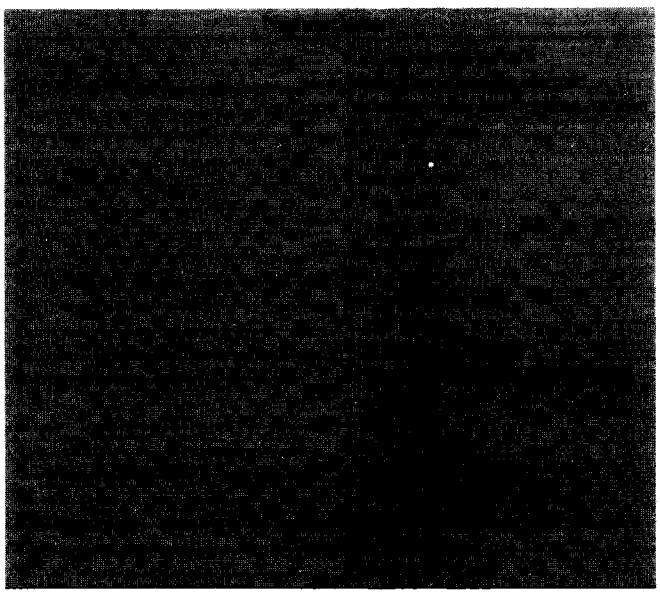

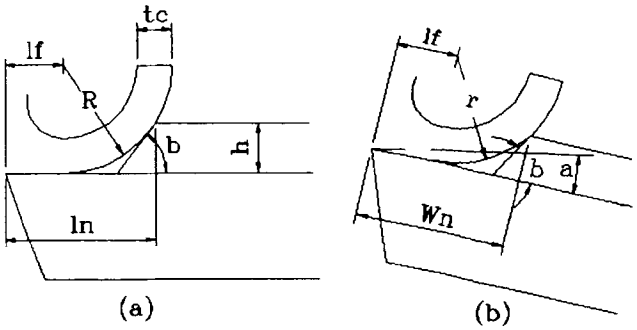

Fig. 1 Formation of the chip in an attached type of chip

Table 1 Chip thickness (t_c)

Cutting speed, m/min	+6° rake angle, mm	– 6° rake angle, mm
50	0.65	0.77
100	0.59	0.60
150	0.47	0.50
200	0.43	0.46
250	0.42	0.43
300	0.37	0.42

Note: Cutting condition: t_o = 0.205 mm; w = 2 mm; back rake angle, –5°; side cutting edge, 15°.

$$R = (w_n - l_f) \times \cot (b / 2) \quad [5]$$

The above two equations are different in form, but the result is the same. Equations 4 and 5 show that four variables affect R, and these consist only of tool geometry and the chip. In these, the components of tool geometry, l_n, h, and b, are acquired easily, but l_f can be obtained by experiment.

2.2.2. *Integral Type*

Equations for the chip radius are derived by use of a similar form to the attached type. It is represented by two equations:

$$R = (l_n - l_f)^2 / 2h + h / 2 \quad [6]$$

$$R = (w_n^2 + l_f^2 - 2 \times w_n \times l_f \times \cos a) / 2w_n \times \sin a \quad [7]$$

These equations produce the same value. Using these results, the chip radius is not affected by the rake angle, but only the chip form is different in cutting.

3. Experiments

To obtain the chip radius, the governing equation of the shear angle is needed. In the current experiments, the governing equation of the shear angle is represented by a relationship of the variation of the shear angle, the cutting speed, and depth of cut.

3.1. *Effect of the Shear Angle and the Chip Breaker*

Table 1 presents the experimental chip thickness for various cutting speeds at a constant depth of cut and a constant width of cut. Table 2 presents the experimental chip thickness for various depths of cut. On the basis of the experiments, to obtain the shear angle for the cutting speed and the depth of cut, the radius of the chip by a chip breaker for an arbitrary cutting speed and depth of cut was measured and analyzed. It was found that l_f approximates the chip thickness, t_c.[6]

Table 2 Chip thickness (t_c)

Depth of cut, mm	+6° rake angle, mm	– 6° rake angle, mm
0.102	0.37	0.36
0.205	0.51	0.54
0.292	0.69	0.74
0.409	0.82	0.86
0.511	1.01	1.03

Note: Cutting condition: V = 100 m/min; w = 2 mm.

Table 3 Specifications of the experimental chip breakers

	Tip 1	Tip 2
h	1.2	1.0
l_n	3.1	3.0

Table 4 Experimental chip radii

Tool	Chip breaker I (integral type)	Chip breaker II (integral type)
PSBN R 2020 K-12		
l_n	3.1	3.0
h	1.2	1.0
Chip		
Radius	6.85	6.70
Thickness	0.55	0.55

Note: Cutting condition: V = 86 m/min (diameter, 24.9 mm; rpm, 1100); t_o = 0.205 mm; w = 2 mm.

Table 3 presents the specifications of the chip breaker used in the current experiment. Table 4 presents the experimental results for the arbitrary cutting conditions. Figures 2 and 3 show the shear angle obtained from the shear angle experiment with a variation in depth of cut and cutting speed. Functions of the first degree simplified from the experimental curve are as follows. First, assuming that the shear angle is a function of the first degree of V, $\varphi = f(V)$, the shear angle φ is $a + b \times V$, i.e., $\varphi = a + b \times V$, where a and b are constants. Also, a and b can be computed by the least-square method.[7] The relationship between φ and V can be written as:

$$\varphi = 15.738 + 0.04801 \times V \text{ (+6° rake angle)} \quad [8]$$

$$\varphi = 14.333 + 0.04659 \times V \text{ (–6° rake angle)} \quad [9]$$

Applying the same method to the curve in Fig. 3 and assuming that the shear angle φ is a function of the first degree of t_o, $\varphi = f(t_o)$. The relationship between φ and t_o can be written as:

$$\varphi = 14.932 + 28.559 \times t_o \text{ (+6° rake angle)} \quad [10]$$

$$\varphi = 15.395 + 24.801 \times t_o \text{ (–6° rake angle)} \quad [11]$$

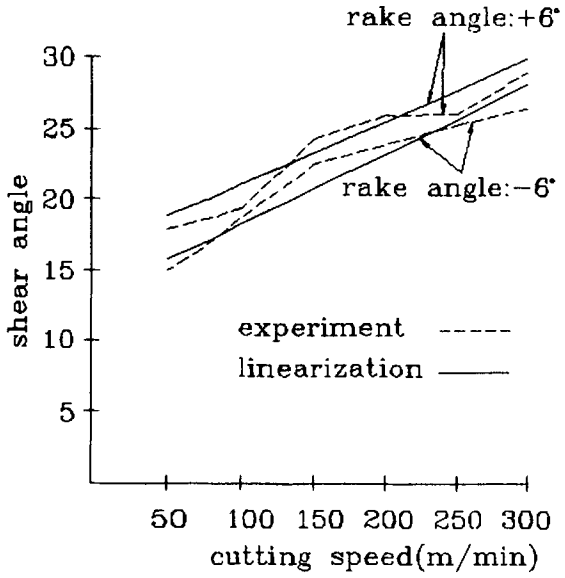

Fig. 2 Change in shear angle with cutting speed.

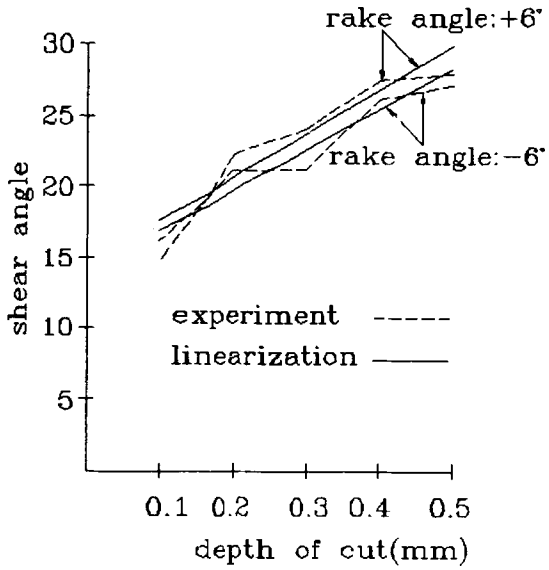

Fig. 3 Change in shear angle with depth of cut.

The solid lines in Fig. 2 and 3 show the linearized relationship. Figure 4 shows the experimental apparatus used for the measurement of horizontal and vertical forces acting on the chip breaker.

3.2. *Analysis of Experimental Results*

Chip radii obtained from the experiment are $R_1 = 3.42$ mm and $R_2 = 3.35$ mm for chip breaker I and II, respectively. Theoretical values of the chip radii are $R_1 = 3.23$ mm and $R_2 = 3.43$ mm for chip breaker I and II, respectively, under cutting conditions in which the cutting speed was 86 m/min, the depth of cut was 0.205 mm, and the cutting tool was a CSBP R2020 K-12. The percentage of error between the theoretical value of the

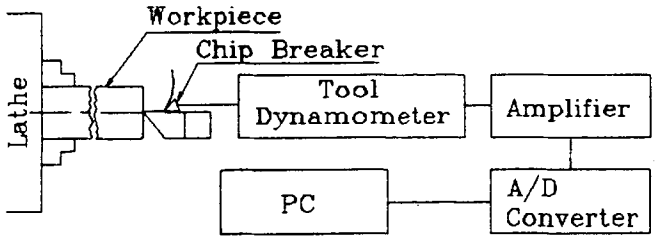

Fig. 4 Schematic of experimental apparatus.

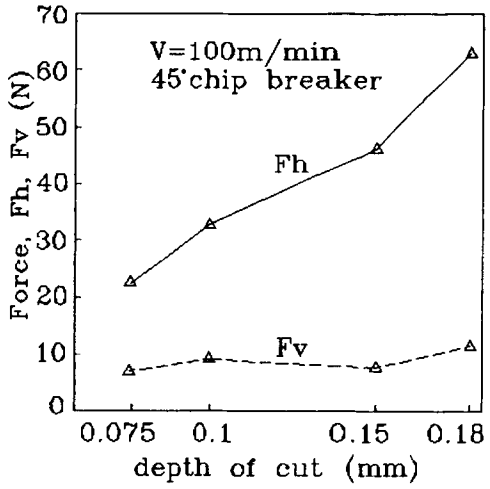

Fig. 5 Effect of depth of cut.

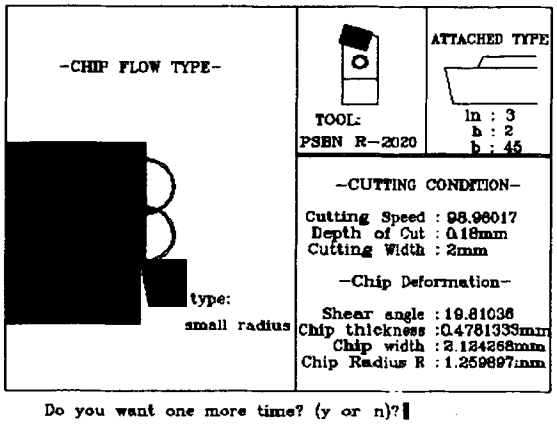

Fig. 6 Simulation of small radius chip.

chip thickness of 0.55 mm and the measured value of 0.58 mm is about 6%. The percentage of error of the chip radius R is about 6% for chip breaker I (theoretical, 6.46 mm; measured, 6.85 mm) and about 5% for chip breaker II (theoretical, 6.86 mm; measured, 6.70 mm). These values are sufficient to verify the theory because the amount of error is very small for the arbitrary cutting conditions. Figure 5 shows the relationship between the depth of cut and the force acting on the chip breaker when the cutting force (100 m/min) and slant angle (45°) are

kept constant. The horizontal force rapidly increases with increases in the depth of cut, but the vertical force remains constant.

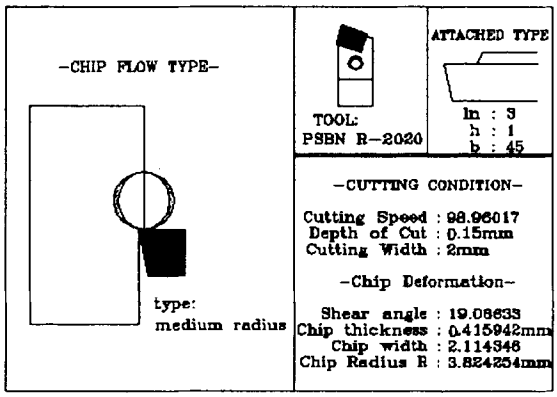

Fig. 7 Simulation of medium radius chip.

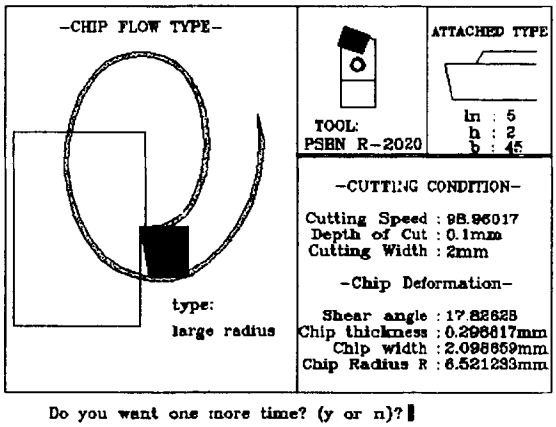

Fig. 8 Simulation of large radius chip.

4. Computer Analysis

4.1. *Simulation*

Using the data obtained from the experiment, a relationship was derived and applied to a computer program. This program calculates the chip radius, classifies the chip flow type, and calculates optimum cutting conditions. Then, representative chip types are selected for a given cutting condition to divide chips into several types. The primary relationship used in classifying the chip flow type is as follows:

Small radius: $r/w_c < 1$

Medium radius: $1 < r/w_c < 2$

Large radius: $r/w_c > 2$ [12]

where r is the radius of the chip, and w_c is the width of the chip.

$$w_c^2 = (w \times \tan(\alpha) + t_o)^2 + w^2 \quad [13]$$

Although this is slightly different from the actual value, it approximates the true value. The simulation algorithm first decides the cutting tool and the cutting conditions. A chip breaker is then selected, and the shape of the chip is simulated on the computer screen (Fig. 6 to 8).

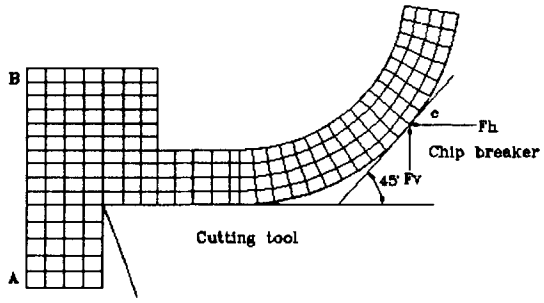

Fig. 9 Configuration of the finite-element model.

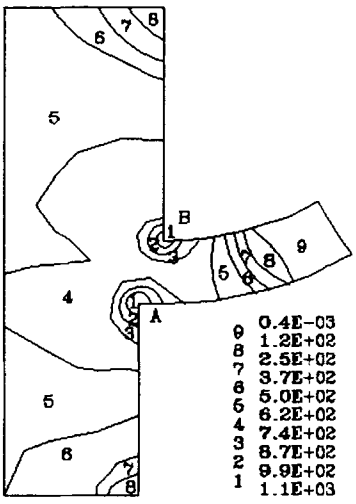

(a) without chip breaker

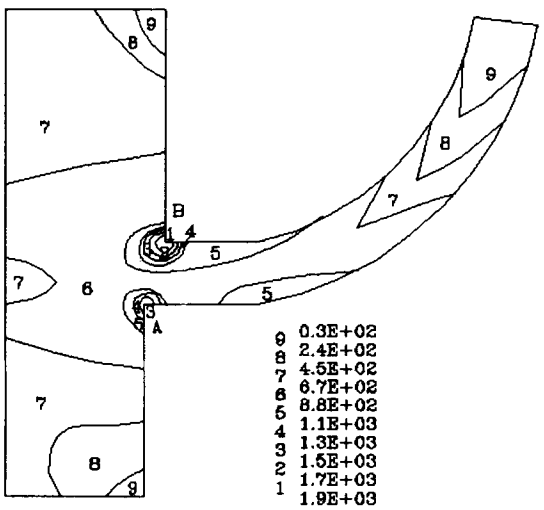

(b) with chip breaker

Fig. 10 Stress distribution of depth of cut of 0.1 mm.

4.2. *Finite-Element Modeling*

The finite-element mesh configuration is shown in Fig. 9. The model consisted of 179 four-node isoparametric elements for the workpiece and chip. The total number of nodes was 225. The workpiece was modeled with a yield strength of 590 N/mm^2. Section AB in Fig. 9 was constrained against displacement in the x-, y- direction. Analysis of the cutting process was performed by simulating the cutting force and chip breaker force on the chip by means of the experiment. To quantify the effect of the plastic characteristics of the workpiece material (SM45C) on the cutting process, an elastic/perfectly plastic constitutive model was considered in this analysis. The general-purpose finite-element program ANSYS (version 4.4) was used to solve the chip breaking problem. A bilinear stress-strain relationship was assumed for the material nonlinearity, whereas yielding was described by the Von Mises yield criterion. To simulate the chip breaking, the Newton-Raphson iterative method and large deformation theorem were used.

5. Results and Discussion

Figure 10 (a) shows the stress distribution before chip breaking, and Fig. 10 (b) shows the stress distribution during chip breaking. These results show that the equivalent stress (1.9×10^3 N/mm^2) of the B zone reaches a large twice that before chip breaking. By suddenly increasing the stress in the B zone, it is possible that the first location of fracture is the B zone. Therefore, chip separation ultimately must involve fracture along a path of separation where the Von Mises equivalent

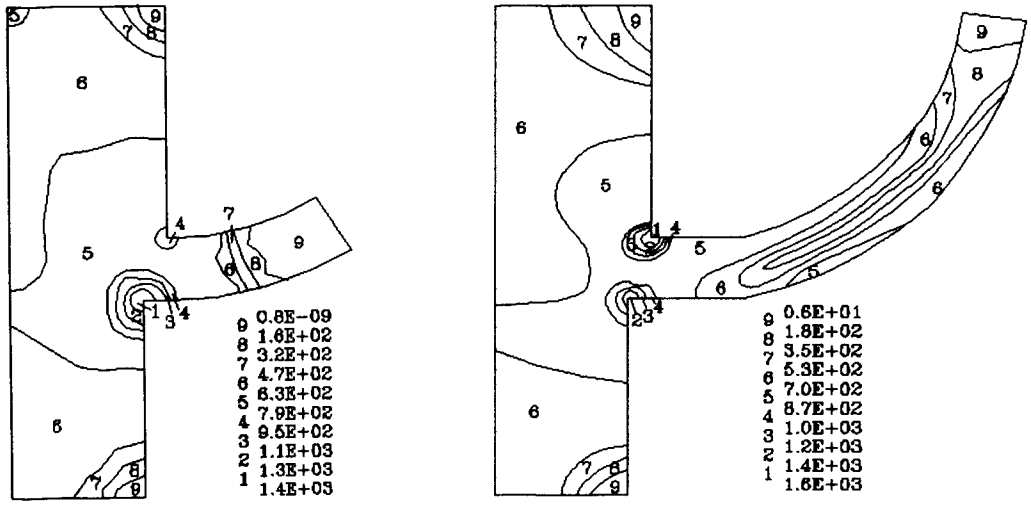

(a) without chip breaker (b) with chip breaker

Fig. 11 Stress distribution of depth of cut of 0.15 mm.

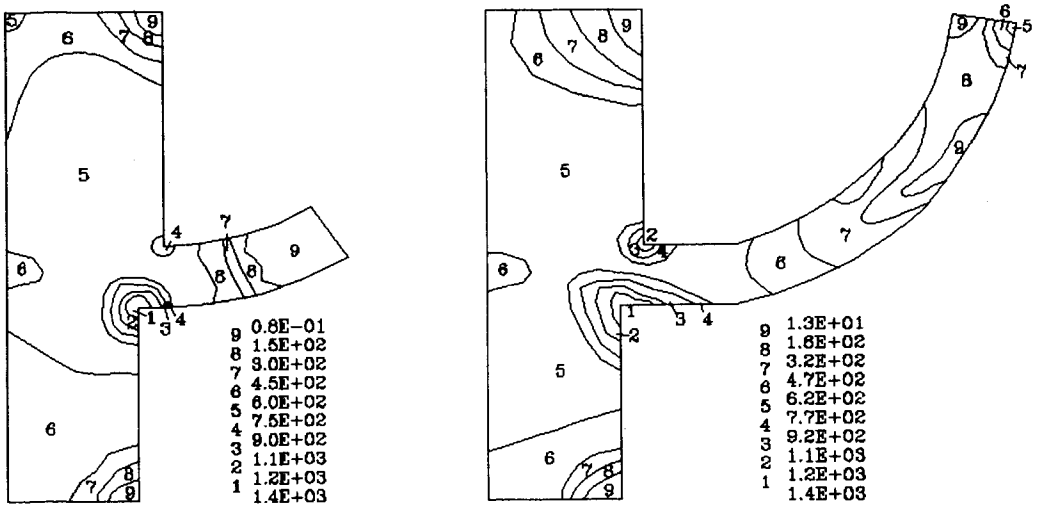

(a) without chip breaker (b) with chip breaker

Fig. 12 Stress distribution of depth of cut of 0.18 mm.

stress reaches a maximum. The higher stresses arise in the shear zone with and without the chip breaker.

Figure 11 shows the results of stress analysis of the depth of cut of 0.15 mm. A tendency to increase stress is similar to that of a depth of cut of 0.1 mm. The equivalent stress is suddenly increased in the B zone, but the amount of increase is smaller than that for the depth of cut of 0.1 mm. The reason for this is the increase in chip thickness in spite of the increase in force acting on the chip breaker. Figure 12 shows the results of stress analysis for a depth of cut of 0.18 mm. From the stress distribution according to the depth of cut, the effect of chip breaking is greater in the case of a thinner chip thickness.

6. Conclusion

The following conclusions can be drawn from the computer analysis. A finite-element model for simulating chip breaking in the orthogonal cutting mode was developed and discussed. Increases in chip radius and a decrease in chip thickness cause a decrease in the force acting on the chip breaker. By simulation, animation of the chip breaking process can be observed on a computer screen. The effect of chip breaking varies with chip thickness.

References

1. K. Nakayama, A Study on Chip Breaker, *Bull. JSME*, Vol 5 (No. 5), 1962, p 142-150
2. K. Nakayama, Chip Control in Metal Cutting, *Bull. Jpn. Soc. Prec. Eng.*, Vol 18 (No. 2), 1984, p 97-103
3. P. Kloor, Coherent SODAR for Automatic Monitoring of the Chip Breaking Process in Turning, *Ann. CIRP*, Vol 34, 1985, p 91-94
4. K. Katbi, Chip Groove, *Cutting Tool Eng.*, 1990, p 59-62
5. M.C. Shaw, Metal Cutting Principles, *Oxford Ser. Advan. Manufact.*, Vol 3, 1984, p 18-46
6. G. Boothroyd, *Fundamentals of Metal Machining and Machine Tools*, MacGraw-Hill, 1975, p 185-195
7. R.W. Hornbeck, *Numerical Method*, Quantum Publishers, 1987, p 121-129